

VIP Transition-Metal Chemistry Very Important Paper

International Edition: DOI: 10.1002/anie.201703235
German Edition: DOI: 10.1002/ange.201703235

A Molecular Boroauride: A Donor–Acceptor Complex of Anionic Gold

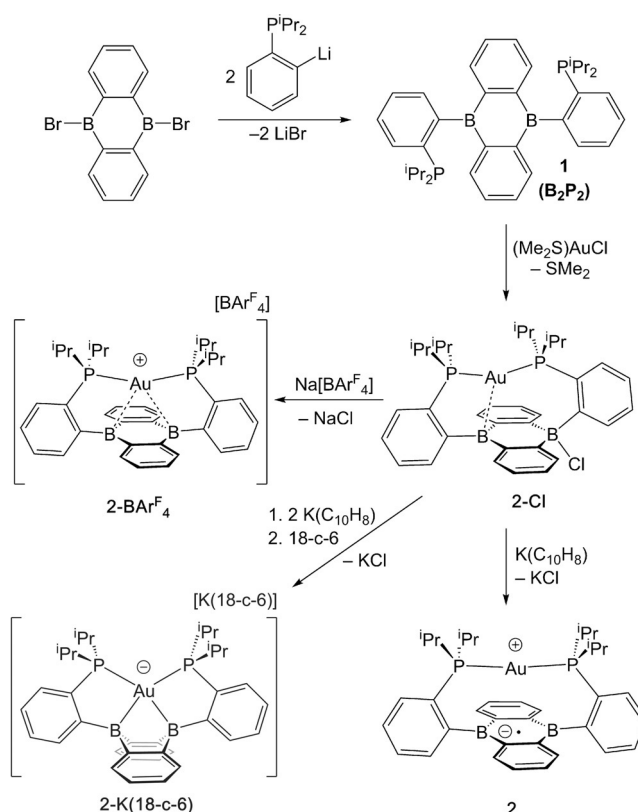
Jordan W. Taylor, Alex McSkimming, Marc-Etienne Moret, and W. Hill Harman*

Abstract: Gold is unique among the transition metals in that it is stable as an isolated anion (auride). Despite this fact, the coordination chemistry of anionic gold is virtually nonexistent, and this unique oxidation state is not readily exploited in conventional solution chemistry owing to its high reactivity. Through the use of a new molecular scaffold based on diboraanthracene (B_2P_2 , **1**), we have overcome these issues by avoiding the intermediacy of zerovalent gold and stabilizing the highly reduced gold anion through acceptor interactions. We have thus synthesized a molecular boroauride $[(B_2P_2)Au]^-$ (**2**) and showed its reversible conversion between Au^{-I} and Au^I states. Through a combination of spectroscopic and computational studies, we show the neutral state to be a Au^I complex with a ligand radical anion. Bonding analyses (NBO and QTAIM) and the isolobal relationship between gold and hydrogen provide support for the description of **2** as a boroauride complex.

The ability to adopt multiple d-electron configurations (and hence oxidation states) is a hallmark of the transition metals,^[1] and much of the chemistry associated with transition-metal complexes, including electron transfer, oxidative addition/reductive elimination, and atom transfer, depends on this phenomenon.^[2] While the transition metals are typically regarded as cation-forming elements, complexes with d-electron counts (d^5 – d^{10}) corresponding to apparent negative oxidation states can be stabilized by electron-accepting ligands such as carbon monoxide and arenes.^[3] In this context, the chemistry of gold is remarkable, as it alone among transition metals is stable as an isolated anion in the condensed phase.^[4] The stability of the 12-valence-electron auride anion (Au^-), such as in the salt $[NMe_4][Au]$,^[5] thus highlights the unusual properties of Au in the context of transition-metal chemistry more generally. Owing in part to the relativistic stabilization of the 6s orbital, the electron affinity of Au (2.3 eV)^[6] is significantly larger than most transition metals and rivals that of the halogens.^[7] Unfortunately, Au^- is only accessible by the direct reaction of metallic

Au with elemental alkali metals such as Cs and Rb, and the solution chemistry of auride compounds is restricted to liquid ammonia.^[8] Furthermore, the intermediacy of Au^0 and its propensity to aggregate into metallic gold^[9] complicates the electrochemical conversion of Au^- to more well-known monometallic gold complexes in positive oxidation states. As a result, a molecular system capable of reversible interconversion between Au^I and Au^{-I} states is unknown.

Intrigued by the possibility of accessing redox chemistry associated with the auride anion in a molecular setting, we began to explore ligand scaffolds capable of circumventing two central problems with a hypothetically reversible Au^I/Au^{-I} system: 1) the potential intermediacy of Au^0 that could lead to the precipitation of elemental gold and 2) the electronically saturated and highly reducing Au^{-I} state, which should require strong acceptor interactions^[10] for stability within a molecular framework. By using concepts including ligand redox-activity and hemilability, respectively, we designed the ligand B_2P_2 (**1**, Scheme 1) to overcome these challenges, which features *trans*-disposed phosphine donors

Scheme 1. Synthesis of the ligand B_2P_2 and its Au complexes.

[*] J. W. Taylor, Dr. A. McSkimming, Prof. W. H. Harman
Department of Chemistry, University of California-Riverside
Riverside, CA 92521 (USA)
E-mail: hill.harman@ucr.edu

Dr. M.-E. Moret
Organic Chemistry & Catalysis
Debye Institute for Nanomaterials Science
Utrecht University, Universiteitsweg 99
3584 CG Utrecht (The Netherlands)

Supporting information and the ORCID identification number(s) for the author(s) of this article can be found under:
<https://doi.org/10.1002/anie.201703235>.

straddling a 9,10-dihydro-9,10-diboraanthracene (DBA) core. Agapie et al. have recently used metal complexes of related noninnocent terphenyl diphosphines for the activation of small molecules, including CO^[11] and O₂.^[12] The phosphine donors are poised to stabilize a linear Au^I cation, while the intrinsic redox activity and Lewis acidity of the DBA core give it the ability to both serve as an electron reservoir and engage in acceptor interactions with a highly reduced metal atom as needed. Herein, we report the synthesis and reversible redox chemistry of [(B₂P₂)Au]ⁿ (**2**ⁿ, *n* = −1, 0, +1), which is isolable in three states of charge. Both the cationic and neutral forms of this molecule possess Au^I centers, with the first reduction event taking place at the DBA core. The anionic form, however, is best described as a bridging boroauride featuring a three-center, two-electron (3c-2e) B–Au–B interaction. Taken together, these results detail a strategy for accessing an unprecedented reversible Au^I/Au^{−I} redox couple in a molecular system.

The diphosphine-DBA ligand **1** is accessed by the addition of two equivalents of 2-diisopropylphosphinophenyllithium to 9,10-dibromo-DBA in toluene. Metalation of **1** with (Me₂S)AuCl in CH₂Cl₂ affords a complex with the stoichiometry [(B₂P₂)Au]Cl (**2-Cl**) in 89% yield. Single-crystal X-ray diffraction (XRD) reveals **2-Cl** to be zwitterionic in the solid state with the chloride anion bound to a tetrahedral boron center (Figure 1, left).^[13] The geometry at the *pseudo*-two-

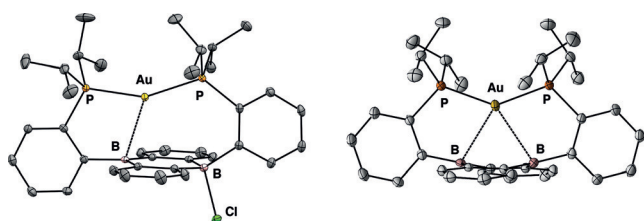


Figure 1. Thermal ellipsoid plots (50%) of [(B₂P₂)Au]Cl (**2-Cl**, left) and the cation in [(B₂P₂)Au][BARF₄] (**2-BARF₄**, right). Unlabeled ellipsoids correspond to carbon. H atoms, counterions, and cocrystallized solvent molecules have been omitted for clarity. Selected bond lengths and angles for **2-Cl**: *d*_{Au–B} = 2.575(2), 3.468(2) Å, ∠P–Au–P = 153.69(2)°; for **2-BARF₄**: *d*_{Au–B} = 2.610(2), 2.678(2) Å, ∠P–Au–P = 141.58(2)°.

coordinate Au^I center is modestly bent (∠P–Au–P = 153.7°) with an intermediate length contact with the second planar, three-coordinate boron atom (*d*_{Au–B} = 2.5645(16) Å). In a 3:1 mixture of THF:benzene, **2-Cl** exhibits a pair of inequivalent and strongly coupled ³¹P resonances by NMR spectroscopy at 57.3 and 53.9 ppm (²*J*_{P–P} = 240 Hz, Figure S6), consistent with the preservation of the zwitterionic form in solution. In CDCl₃, however, a single ³¹P resonance is observed for **2-Cl** at 57.1 ppm (Figure S5), suggesting either complete chloride dissociation or its rapid exchange between the two boron sites.

Anion metathesis of **2-Cl** with Na[BARF₄] (Ar^F = 3,5-bis(trifluoromethyl)phenyl) gives the complex salt [(B₂P₂)Au][BARF₄] (**2-BARF₄**) (Scheme 1). The single-crystal XRD structure of **2-BARF₄** reveals a symmetrical [(B₂P₂)Au]⁺ cation (**[2]⁺**) with a significantly bent P–Au–P linkage (∠P–Au–P = 141.6°) that situates the gold center within 2.7 Å of each

boron atom (*d*_{Au–B} = 2.6101(17), 2.6785(18) Å) (Figure 1, right). While long, these Au–B distances are consistent with those observed in related Au^I borane complexes for which weak donor acceptor interactions are thought to exist.^[14] Given the electron deficiency of the central C₄B₂ ring of the DBA core, this interaction in **[2]⁺** can be viewed as an inverse cation–π interaction, wherein an electron-rich cation interacts with an electron deficient π-system.

Cyclic voltammetry performed on **2-BARF₄** (0.1 M [NBu₄][PF₆] in CH₃CN, 100 mV s^{−1} scan rate) revealed two reversible redox processes at −1.60 and −2.05 V versus Fc/Fc⁺ (Fc = (C₅H₅)₂Fe, Figure 3A). By comparison, the gold-free DBA derivative 9,10-Mes₂-DBA (Mes = 2,4,6-trimethylphenyl),^[15] a proxy for the DBA core in **[2]⁺**, undergoes reversible reduction events at −1.62 and −2.48 V versus Fc/Fc⁺ under these conditions.^[16] While the first reduction of **[2]⁺** occurs at a potential comparable to that of its gold-free analog, the second reduction is positively shifted by over 400 mV relative to 9,10-Mes₂-DBA. These data imply a crucial role for Au in the observed redox chemistry of the [(B₂P₂)Au] platform (Figure 2).

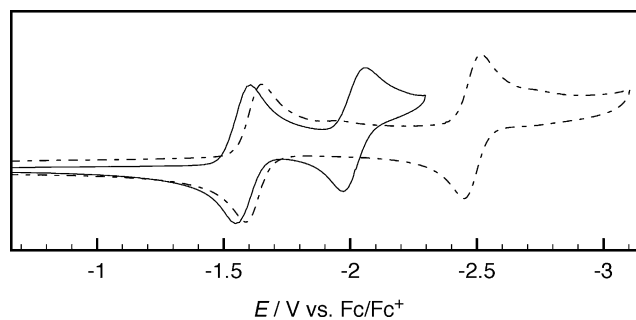


Figure 2. Normalized cyclic voltammograms of [(B₂P₂)Au][BARF₄] (solid) and 9,10-Mes₂-DBA (dashed) carried out in CH₃CN with 0.1 M [Bu₄N][PF₆] supporting electrolyte at a scan rate of 100 mV s^{−1}.

To understand roles of both the Au center and the DBA core in the redox chemistry of [(B₂P₂)Au], especially the remarkable anodic shift in the second reduction event, we sought to isolate and characterize the one- and two-electron reduced products. Chemical reduction of **2-Cl** with 1 equivalent of K(C₁₀H₈) in THF gives the neutral radical (B₂P₂)Au (**2**) as a purple crystalline solid (Scheme 1). The solid-state structure of **2** was determined by XRD and features a slightly bent diphosphine–gold moiety (∠P–Au–P = 158.97(2)°) spanning a planar DBA core (Figure 3, left). In contrast to **[2]⁺**, the Au–B interactions in **2** are lengthened substantially (*d*_{Au–B} = 3.013(2) and 3.084(3) Å). The ¹H NMR spectrum of **2** is consistent with paramagnetism (Figure S11), and the X-band electron paramagnetic resonance (EPR) spectrum of **2** in fluid 2-methyltetrahydrofuran (2-MeTHF) reveals a broad triplet centred at *g* = 1.99 (Figure 4, left). The observed feature is consistent with hyperfine interactions with two equivalent ³¹P nuclei (*I* = 1/2, *A*_{iso}(³¹P) = 55 MHz), and while this signal broadens upon cooling to 100 K, no additional fine structure was resolved (Figure S22). Although the ³¹P hyperfine interactions in **2** could be taken to indicate significant spin density (and hence reduction) at Au, the established

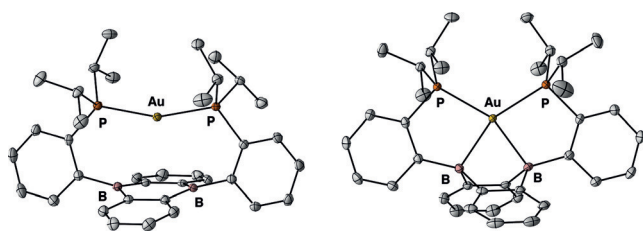


Figure 3. Thermal ellipsoid plots (50%) of $(\text{B}_2\text{P}_2)\text{Au}$ (**2**, left), and the anion in $[(\text{B}_2\text{P}_2)\text{Au}][\text{K}(18\text{-c-6})]$ ($[\mathbf{2}]^-$, right). Unlabeled ellipsoids correspond to carbon. H atoms, counterions, and cocrystallized solvent molecules have been omitted for clarity. Selected bond lengths and angles for **2**: $d_{\text{Au-B}} = 3.013(2)$, $3.084(3)$ Å, $\angle \text{P-Au-P} = 158.97(2)^\circ$; for $[\mathbf{2}]^-$: $d_{\text{Au-B}} = 2.237(2)$, $2.241(3)$ Å, $\angle \text{P-Au-P} = 118.87(3)^\circ$.

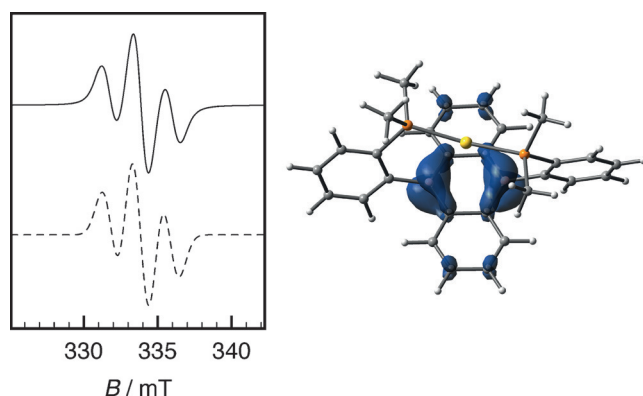


Figure 4. Left: X-band EPR spectrum (9.309 GHz) of $(\text{B}_2\text{P}_2)\text{Au}$ collected in 2-MeTHF solution at 298 K (solid) along with its simulation (dashed). Simulation parameters are $g = 1.99215$ and $A_{\text{iso}}(^{31}\text{P}) = [56.5, 56.5]$ MHz with a linewidth of 1.54 mT. Right: spin-density plot for a truncated model of **2** calculated by DFT (see the Supporting Information for details).

redox chemistry of DBA derivatives and lack of precedent for authentic coordination complexes of $\text{Au}^{0[17]}$ suggest that **2** is best formulated as a zwitterion containing a Au^{I} cation linked to a DBA radical anion. Indeed, DFT calculations performed on a slightly truncated^[18] model suggest that the spin density of **2** is localized primarily on the DBA core (Figure 3, right), with natural spin populations of $0.26 e^-$ on each boron and most of the remaining spin delocalized over the carbon atoms of the DBA unit (see the Supporting Information). This electronic structure nonetheless gives rise to a significant calculated hyperfine interaction (via the IGLO method, see the Supporting Information for details)^[19] with the ^{31}P nuclear spins (calc. $A_{\text{iso}}(^{31}\text{P}) = 37.0$ MHz) and much smaller boron hyperfine interactions (calc. $A_{\text{iso}}(^{11}\text{B}) = 9.7$ MHz) in qualitative agreement with the experimental spectrum. The large, isotropic ^{31}P hyperfine interaction is presumably mediated by hyperconjugation^[20] either through the phenylene linker or the Au center. In either case, very small spin densities at ^{31}P can lead to large EPR hyperfine interactions so long as there is significant involvement of the 3s orbital on P.^[21] To wit, the natural spin density at each P atom is calculated to be approximately $0.005 e^-$ for **2**, 43 % of which is hosted in the 3s orbital. From a structural perspective, the lengthening of the

Au–B distances in **2** is consistent with the population of the DBA-based orbital that served as the acceptor for the weak interaction observed in $[\mathbf{2}]^+$.

Reduction of **2-Cl** with 2 equivalents of $\text{K}(\text{C}_{10}\text{H}_8)$ gives the diamagnetic crimson anion $[(\text{B}_2\text{P}_2)^{\text{iPr}}\text{Au}]^-$ ($[\mathbf{2}]^-$), which features a sharp singlet in its ^{11}B NMR spectrum at 11.1 ppm, a significant upfield shift relative to the broad feature at 32.0 ppm observed for $[\mathbf{2}]^+$. Addition of 18-crown-6 (18-c-6) to the reaction mixture affords crystals of the complex salt $[(\text{B}_2\text{P}_2)^{\text{iPr}}\text{Au}][\text{K}(18\text{-c-6})]$ (**2-K(18-c-6)**). Single crystal XRD on this material reveals a dramatic rearrangement of the $\text{B}_2\text{P}_2\text{Au}$ core, with very short Au–B distances ($d_{\text{Au-B}} = 2.241(2)$, $2.237(2)$ Å) and pyramidalized boron centers ($\Sigma \angle \text{C-B-C} = 343.8^\circ$, 343.9°) (Figure 3, right). Although complexes with gold–borane donor–acceptor interactions have been reported, they typically feature a Au^{I} donor to a single borane acceptor and longer Au–B distances in the range of 2.3–2.9 Å. In contrast, $[\mathbf{2}]^-$ is formally composed of an auride anion interacting with two *cis*-disposed borane ligands and is the only example of a mononuclear transition metal complex featuring two such short metal–organoborane (BR_3) interactions. The short Au–B distances in $[\mathbf{2}]^-$ are comparable to those found in gold complexes featuring base-stabilized boryl^[22] and borylene^[23] ligands, multimetallic boride complexes,^[24] as well as metal–laborane cluster compounds.^[25]

There are in principle two qualitative descriptions of the B–Au–B bonding in $[\mathbf{2}]^-$, either as two, two-center, two-electron (2c-2e) bonds or a single three-center, two-electron (3c-2e) bond. Given the well-established isolobal relationship between gold and hydrogen^[26] we favor the latter description wherein $[\mathbf{2}]^-$ is understood as a donor–acceptor complex between an auride anion and DBA. Thus $[\mathbf{2}]^-$ is analogous to a borohydride, and would therefore be described as a bridging borauride ($[\text{R}_3\text{B}(\mu\text{-Au})\text{BR}_3]^-$). We stress the plausibility of the auridic description of the gold center in $[\mathbf{2}]^-$ by emphasizing that Au is stable in anionic form and significantly more electronegative than hydrogen ($\chi_{\text{Au}} = 2.54$ and $\chi_{\text{H}} = 2.20$ on the Pauling Scale). In fact, the Au atom is the most electronegative atom in $[\mathbf{2}]^-$. We also highlight that the tetraauridoborate anion ($[\text{BAu}_4]^-$) has been explored computationally and found to exhibit significant similarities with the tetrahydridoborate anion ($[\text{BH}_4]^-$).^[27]

Further insight into this question was provided by DFT calculations on a model of $[\mathbf{2}]^-$.^[18] A quantum theory of atoms in molecules (QTAIM)^[28] analysis of the calculated electron density reveals a straight bond path connecting the Au center to each B atom (Figure 5A). Interestingly, the corresponding bond critical point (BCP) is found in a negative region of the Laplacian, that is, a region with local accumulation of electron density, indicative of a strongly covalent interaction, which sets it apart from typical coordination bonds such as the P–Au interaction in the same compound. In addition, a natural bond orbital (NBO)^[29] analysis reveals that the Au atom and the two B atoms engage in a 3c-2e bond, akin to that found in hydride-bridged boranes such as B_2H_6 , which is described by one filled (τ) and two empty ($\tau^*(\pi)$ and $\tau^*(\Delta)$) orbitals formed by linear combinations of the 6s(Au) with two boron-centered hybrid orbitals of mostly p character ($\text{sp}^{9.3}$: 90.3 % p, 9.7 % s) (Figure 5B). The filled τ orbital arises from a fully in-phase

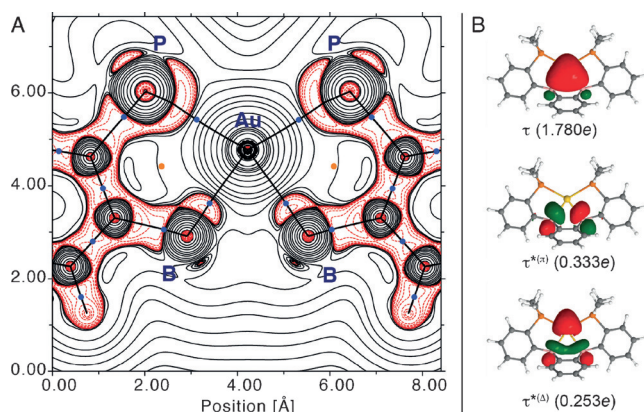


Figure 5. Computational analysis of the Au–B interaction. A) Contour map (negative values in dashed red) of the Laplacian distribution $\nabla^2\rho(r)$ in the B–Au–B plane. Bond paths are depicted as black lines, bond (BCP) and ring (RCP) critical points as blue and orange circles, respectively. B) Natural bonding orbitals (NBOs) describing the B–Au–B three-center/two-electrons bond and their electronic population (in parenthesis).

combination (37.6% Au, $2 \times 31.2\%$ B); the $\tau^{*(\pi)}$ orbital has a nodal plane containing the Au atom and is purely boron-centered, while the $\tau^{*(\Delta)}$ orbital has a nodal surface containing both boron atoms and consists of 62.4% $6s(\text{Au})$ and $2 \times 18.8\%$ $sp^{9,3}(\text{B})$. Two main delocalization effects are identified by second-order perturbation theory. First, a strong donation from P-centered lone pairs into the $\tau^{*(\Delta)}$ orbital (57.1 kcal mol $^{-1}$) describes the expected P \rightarrow Au dative bonds. Second, the in-plane d-orbital of Au is somewhat delocalized into the $\tau^{*(\pi)}$ orbital (31.4 kcal mol $^{-1}$). Taken together, these data support the description of **[2]** $^-$ as a borauride compound.

Interestingly, the covalent bonding picture of the [B–Au–B] $^-$ linkage arising from NBO analysis contrasts with the more ionic description obtained for the [B–Cu] $^-$ unit in the related [(TPB)Cu] $^-$ anion (TPB = tris[2-(diisopropylphosphino)phenyl]borane).^[30,31] There, the bonding electron pair principally resides on the boron atom and engages in a dative bond with the copper center, and the compound is best described as a boron(I) dianion stabilized by coordination to a Cu I center rather than an authentic cupride. This is likely a consequence of the comparatively higher electronegativity ($\chi_{\text{Au}} = 2.54$; $\chi_{\text{Cu}} = 1.9$) and electron affinity ($\text{EA}_{\text{Au}} = 2.3$ eV; $\text{EA}_{\text{Cu}} = 1.2$ eV)^[32] of gold, highlighting its unique ability among transition metals to afford a molecular complex derived from an $d^{10}s^2$ electronic configuration.

In conclusion, through the use of a ligand capable of both redox activity and strong acceptor interactions, we have synthesized a coordination complex of the auride anion and showed its reversible interconversion between Au I and Au $^{-I}$ states. The strategy outlined herein provides a blueprint for unlocking the redox chemistry of auride in mild solution-based processes. Access to an auride equivalent under such conditions may have significant implications for both molecular catalysis and nanotechnology, given the importance of gold chemistry to both fields and ongoing studies are aimed at realizing these goals.

Acknowledgements

We thank the University of California, Riverside for financial support of this work and Dr. Fook Tham for assistance with X-ray crystallographic studies. W.H.H. is a member of the UCR Center for Catalysis. M.-E. M. acknowledges funding from Utrecht University (Tenure-track grant, Sectorplan Natuur-en Scheikunde). The DFT work was carried out on the Dutch national e-infrastructure with the support of the SURF Foundation.

Conflict of interest

The authors declare no conflict of interest.

Keywords: boron · donor–acceptor systems · electrochemistry · gold · ligand design

How to cite: *Angew. Chem. Int. Ed.* **2017**, *56*, 10413–10417
Angew. Chem. **2017**, *129*, 10549–10553

- [1] A. D. McNaught, M. Nic, J. Jirat, A. Wilkinson, *IUPAC Compendium of Chemical Terminology*, 2nd ed. (the “Gold Book”), Blackwell Scientific Publications, Oxford, **1997**.
- [2] F. A. Cotton, G. Wilkinson, C. A. Murillo, M. Bochmann, *Advanced Inorganic Chemistry*, 6th ed., Wiley-Interscience, New York, **1999**.
- [3] J. E. Ellis, *Inorg. Chem.* **2006**, *45*, 3167–3186.
- [4] M. Jansen, *Chem. Soc. Rev.* **2008**, *37*, 1826–1835.
- [5] P. D. C. Dietzel, M. Jansen, R. W. Schmutzler, A. J. Bard, M. Jansen, *Chem. Commun.* **2001**, 621, 2208–2209.
- [6] T. Andersen, H. K. Haugen, H. Hotop, *J. Phys. Chem. Ref. Data* **1999**, *28*, 1511.
- [7] M. Jansen, *Solid State Sci.* **2005**, *7*, 1464–1474.
- [8] H. Nuss, M. Jansen, *Angew. Chem. Int. Ed.* **2006**, *45*, 4369–4371; *Angew. Chem.* **2006**, *118*, 4476–4479.
- [9] N. T. K. Thanh, N. Maclean, S. Mahiddine, *Chem. Rev.* **2014**, *114*, 7610–7630.
- [10] A. Amgoune, D. Bourissou, *Chem. Commun.* **2011**, 47, 859–871.
- [11] J. A. Buss, T. Agapie, *Nature* **2016**, 529, 72–75.
- [12] K. T. Horak, T. Agapie, *J. Am. Chem. Soc.* **2016**, *138*, 3443–3452.
- [13] CCDC 1504402, 1504403, 1504404 and 1504405 contain the supplementary crystallographic data for this paper. These data can be obtained free of charge from The Cambridge Crystallographic Data Centre.
- [14] S. Bontemps, G. Bouhadir, K. Miqueu, D. Bourissou, *J. Am. Chem. Soc.* **2006**, *128*, 12056–12057.
- [15] C. Reus, S. Weidlich, M. Bolte, H.-W. Lerner, M. Wagner, *J. Am. Chem. Soc.* **2013**, *135*, 12892–12907.
- [16] C. Hoffend, M. Diefenbach, E. Januszewski, M. Bolte, H.-W. Lerner, M. C. Holthausen, M. Wagner, *Dalton Trans.* **2013**, 42, 13826–13837.
- [17] a) D. S. Weinberger, M. Melaimi, C. E. Moore, A. L. Rheingold, G. Frenking, P. Jerabek, G. Bertrand, *Angew. Chem. Int. Ed.* **2013**, *52*, 8964–8967; *Angew. Chem.* **2013**, *125*, 9134–9137; b) C. R. Landis, R. P. Hughes, F. Weinhold, *Organometallics* **2015**, *34*, 3442–3449.
- [18] Calculations were performed on model systems in which the isopropyl substituents on phosphorus were replaced with methyl groups. See the Supporting Information.
- [19] W. Kutzelnigg, U. Fleischer, M. Schindler, *The IGLO-Method: Ab Initio Calculation and Interpretation of NMR Chemical Shifts*

- and *Magnetic Susceptibilities*, Vol. 23, Springer, Heidelberg, **1990**.
- [20] J. R. Bolton, A. Carrington, A. D. McLachlan, *Mol. Phys.* **1962**, 5, 31–41.
- [21] B. T. Allen, A. Bond, *J. Phys. Chem.* **1964**, 68, 2439.
- [22] D. A. Ruiz, G. Ung, M. Melaimi, G. Bertrand, *Angew. Chem. Int. Ed.* **2013**, 52, 7590–7592; *Angew. Chem.* **2013**, 125, 7739–7742.
- [23] L. Kong, R. Ganguly, Y. Li, R. Kinjo, *Chem. Sci.* **2015**, 6, 2893–2902.
- [24] H. Braunschweig, W. C. Ewing, T. Kramer, J. D. Mattock, A. Vargas, C. Werner, *Chem. Eur. J.* **2015**, 21, 12347–12356.
- [25] A. J. Wynd, A. J. McLennan, D. Reed, A. J. Welch, *J. Chem. Soc. Dalton Trans.* **1987**, 2761–2768.
- [26] a) H. G. Raubenheimer, H. Schmidbaur, *Organometallics* **2012**, 31, 2507–2522; b) T. J. Robilotto, J. Bacsa, T. G. Gray, J. P. Sadighi, *Angew. Chem. Int. Ed.* **2012**, 51, 12077–12080; *Angew. Chem.* **2012**, 124, 12243–12246.
- [27] D.-Z. Li, S.-D. Li, *Int. J. Quantum Chem.* **2011**, 111, 4418–4424.
- [28] R. F. W. Bader, *Chem. Rev.* **1991**, 91, 893–928.
- [29] F. Weinhold, C. R. Landis, *Valency and Bonding: A Natural Bond Orbital Donor-Acceptor Perspective*, Cambridge University Press, Cambridge, **2005**.
- [30] M.-E. Moret, L. Zhang, J. C. Peters, *J. Am. Chem. Soc.* **2013**, 135, 3792–3795.
- [31] E. Kusevska, M. M. Montero-Campillo, O. Mó, M. Yáñez, *Angew. Chem. Int. Ed.* **2017**, 56, 6788–6792; *Angew. Chem.* **2017**, 129, 6892–6896.
- [32] R. C. Bilodeau, M. Scheer, H. K. Haugen, *J. Phys. B* **1998**, 31, 3885–3891.

Manuscript received: March 28, 2017

Accepted manuscript online: June 6, 2017

Version of record online: June 27, 2017